Proceedings World Geothermal Congress 2005
Antalya, Turkey, 24-29 April 2005

Numerical Simulation of Hydraulic Shearing in Fractured Reservoir

Kazuhiko Tezuka, Tetsuya Tamagawa and Kimio Watanabe

1-2-1 Hamada, Mihama-ku, Chiba, 261-0025, Japan

tezuka@rc.japex.co.jp

Keywords: HDR, stimulation, fracturing, injection, simulation, modeling, shearing

ABSTRACT

The numerical simulator "SHIFT", which simulates performances of fractured basement reservoirs during hydraulic stimulations, has been developed. Hydraulic injections are commonly conducted in geothermal reservoirs for a purpose of reservoir stimulation. This treatment is studied vigorously in Hot Dry Rock (HDR) geothermal programs and many success stories are reported. This treatment uses a large volume of slick water with no proppant. The mechanism of permeability enhancement is recognized as shear dilation, which is associated with shear sliding induced by elevated fluid pressure. Once sliding occurs along a pre-existing fracture, asperities of the fracture keep the opening along the plane (self-propping) to maintain permeability. SHIFT simulates the shearing of fractures and the relating permeability change in a dynamic process by coupling the fluid flow analysis and the shear dilation analysis. The simulation is based on a discrete fracture network model, in which pressure distribution and permeability enhancements are calculated simultaneously. The output includes a history of injection pressure, microseismic (AE) activity relating to the shearing along pre-existing fractures.

The paper describes the concept of the SHIFT and its performance by showing results of the case study for the fractured basement reservoir in Hokkaido, Japan.

1. INTRODUCTION

Hydraulic fracturing is widely used as reservoir stimulation technique for a purpose of productivity and/or injectivity enhancement in geothermal wells and many success stories are reported (Tester et al., 1989; Gerard, et al., 1997; Nagai and Tenma, 1997). The technique is slightly different from the conventional hydraulic fracturing commonly used in oil/gas industries. Slick water with no proppant agents is used as an injection fluid. Studies in Hot Dry Rock (HDR) geothermal programs revealed that the mechanism of permeability enhancement is caused by shear dilation, which is induced by elevated fluid pressure. In shear dilation, the predominate mode of fracturing is shear sliding (mode-II), instead of opening (mode-I). Once sliding occurs along a pre-existing fracture or a plane of weakness, natural mismatches and asperities could keep the opening along the plane (self-propping) to maintain permeability (Ito and Hayashi, 2003). Microseismic monitoring, which is well developed in HDR geothermal fields, clearly show volumetric growth of the stimulated region (Baria and Green, 1986; House, 1987; Talebi and Cornet, 1987;Beauce et al., 1995, Jupe et al., 1992; Wallroth et al., 1996, Sasaki, 1998). Analyzed microseismic mechanisms have proven the fact that shear sliding had been certainly happening at the fracture planes (Pearson, 1981; Pine and Batchelor, 1984; Tezuka and Niitsuma, 2000).

Modeling of hydraulic fracturing focusing the shear dilation was first presented by Willis-Richards et al. (1996). Then, several case studies to investigate the mechanism of volumetric growth of the reservoir in HDR test sites were reported by applying and modifying this modeling scheme (Narayan et al., 1998; Jing et al., 2000). However, the modeling code "FRACSIM" can treat only a steady state injection with a constant injection rate. An output from the modeling is a stimulated region, which has reached the equilibrium in an interaction between a state of stress, an injection pressure, and leakage of injected fluid toward outer boundary. To design the optimal injection schedule the simulator should have a function to treat shear dilation in a dynamic process.

This paper presents a new numerical simulator "SHIFT", which can simulate shear dilation in a dynamic process, taking into account an injection history and a total amount of injected water. The simulator also includes a function to handle two kind of fluid (i.e. water and gas) so as to expand its applicability to oil/gas reservoirs.

2. SIMULATOR "SHIFT"

SHIFT consists of four major routines, "input", "continua conversion", "flow analysis" and "shearing analysis". The flow diagram of these routines is shown in Figure 1, and their functions are described below.

2.1 Fracture Model Input Routine

Information obtained by field measurements is put into the simulator though a discrete fracture network model (DFN model, Tezuka and Watanabe, 2000). In a DFN model each fracture is assumed to be a parallel-sided circular plate, and is specified with center point, radius, aperture, dip, dip-azimuth and some optional parameters. The other input parameters for simulation include in-site stress state, rock and fluid properties, and fracture related propertires as listed in Table 1 and 2.

2.2 Equivalent-continua Conversion Routine

It is not practical to analyze fluid flow in each individual fractures for the DFN model, which includes a large number of fractures. Therefore, the permeability distribution associated with the fractures is converted to that of an equivalent-continua. In numerical calculations, the model volume is divided into a mesh of small elements, and the local permeability is given between the elements where fractures intersect the element interfaces as shown in Figure 2. The local fluid flow is calculated based on the cubic-law, expressed by the following equation,

$$Q = w \cdot \frac{a_e^3}{\mu} \cdot \frac{\Delta P}{d} \tag{1}$$

where Q is volumetric quantity of fluid, w is fracture length at element interface, a_e is hydraulic-effective fracture

aperture, μ , ΔP and d are viscosity, pressure and the distance between the elements. Figure 3 illustrates this concept.

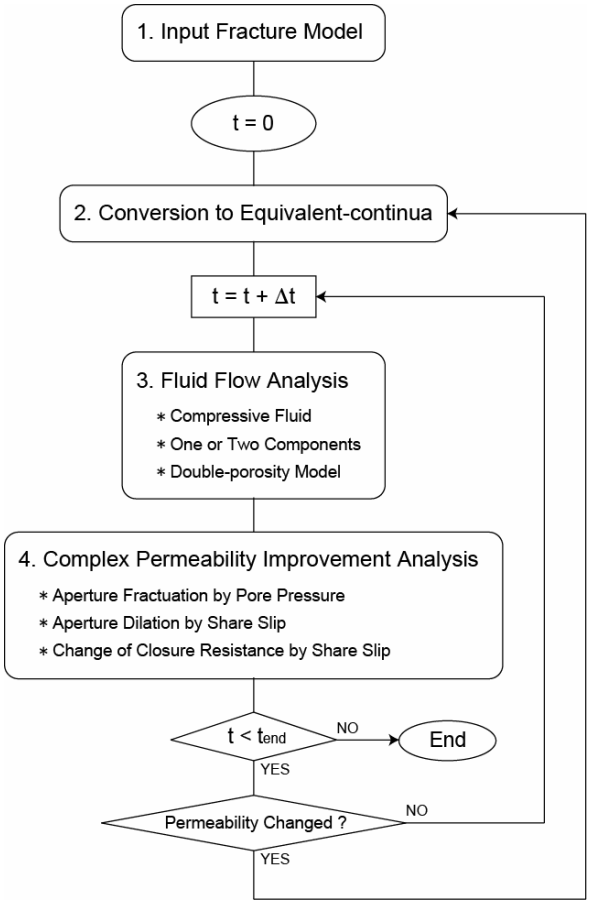

Figure 1: Flow chart of numerical simulator "SHIFT".

2.3 Fluid Flow Analysis Routine

SHIFT analyzes one or two components of fluid. The flow of each component is expressed by following equation.

$$\mu_i \cdot \phi \cdot c_i \cdot \frac{\partial}{\partial t}(P \cdot S_i) = K_x(P) \cdot k_i(S_i) \cdot \frac{\partial^2 P}{\partial x^2} + K_y(P) \cdot k_i(S_i) \cdot \frac{\partial^2 P}{\partial y^2} + K_z(P) \cdot k_i(S_i) \cdot \frac{\partial^2 P}{\partial z^2} \quad (2)$$

where ϕ is reservoir porosity. K represent the absolute permeability in the x, y and z directions. k_i, S_i and c_i express the relative permeability, volumetric ratio and compressibility of component i, respectively. Equation (2) is formed for each element, and the pressure distribution can be obtained by solving these simultaneous equations numerically. SHIFT can also handle the double-porosity model for fluid flow analysis.

2.4 Permeability Improvement Analysis Routine

The fracture aperture changes based on the effective normal stress on the fracture surface, σ_n', which can be obtained from normal stress on the fracture surface σ_n, and pore pressure P_F, following the equation below.

$$\sigma_n' = \sigma_n - P_F \quad (3)$$

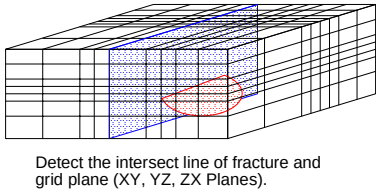

Figure 2: Fracture permeability conversion to equivalent-continua.

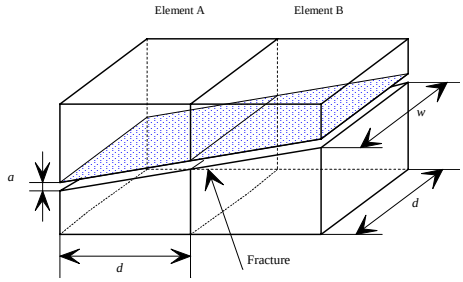

Figure 3: Permeability evaluation between elements.

The fracture aperture, a, is assumed to be calculated by the following equation in SHIFT.

$$a = \frac{A}{1 + 9 \cdot \frac{\sigma_n'}{B}} \cdot a_0 \quad (4)$$

a_0 is the standard aperture without normal stress, i.e. $\sigma_n' = 0$. A is the constant that takes $A = 1$ before the fracture makes shear slip, and $A > 1$ depending on aperture dilation after slipped. A fracture that satisfies the following stress condition is considered to make shear slip.

$$\tau \geq \mu \cdot \sigma_n' \quad (5)$$

B is "90% closure stress" which implies the closure resistance of fracture. A behavior of the fracture aperture with respect to the effective normal stress is shown in Figure 4.

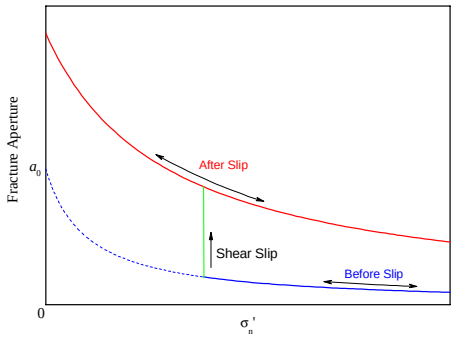

Figure 4: Fracture aperture as a function of effective normal stress.

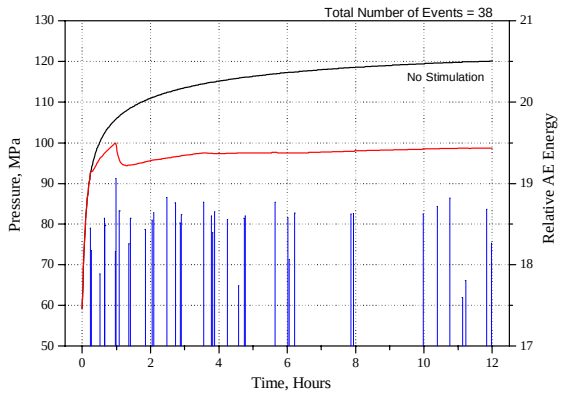

(a) Histories of injection pressure and AE event

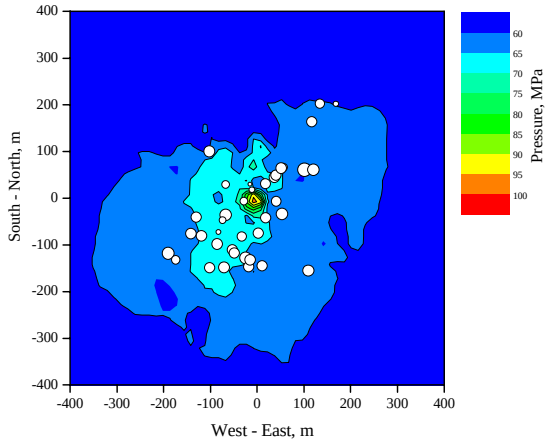

(b) Pressure distribution and AE event locations

Figure 5: Examples of outputs of SHIFT. Upper graph (a) shows histories of injection pressure and AE event occurrences. Lower contour (b) shows pressure distribution and AE event locations.

2.5 Outputs

Typical outputs from SHIFT are the reservoir pressure and the shearing information. Because of the computer's storage limitation, only injection pressure is recorded as a continuous data. Pressure distribution of the whole reservoir model is recorded at certain time points specified in the input parameters. The fracture shearing information, such as slip time and slip location, is instantly outputted. The magnitude of radiated elastic energy (termed relative AE magnitude, M) is also calculated by the following equation and is added to the shear information file.

$$M = \log\left[\int_{\Sigma}\left\{\left(1-\frac{f_d}{f_s}\right)\cdot\tau\right\}\right] \qquad (5)$$

where f_d and f_s are dynamic and static friction coefficients, and τ is shear stress acting to the fracture surface. Σ is considered as a fracture area. Conceptual diagrams of these outputs are shown in Figure 5.

3. CASE STUDIES

3.1 Hydraulic injection into gas saturated reservoir

This section presents a case study applying SHIFT to a numerical simulation for the hydraulic injection experiment in the Yufutsu gas reservoir, Hokkaido island, northern Japan. The reservoir extends over a depth range of 4,000 to 5,000 meters and is comprised of Cretaceous granite overlain by an alluvial/fluvial conglomerate of Eocene age, in which fracture network is well-developed. Although the reservoir rock itself has very low porosity and permeability, the well-developed fracture network plays roles as the reserve space and the flow pathways.

The objective of the experiment was to investigate a possibility of inducing shearing by water injection into the gas saturated reservoir and to see an AE activity and corresponding changes of injectivity/productivity of the well. The pumping period consists of three stages, i.e. the 1st step-rate injection, the constant high-rate injection followed by a shut-in period of 12 hours, and the 2nd step-rate injection. The two step rate injection periods include exactly the same pumping schedule.

Figure 6 summarizes the pumping history and AE activity during the injection experiment. The blue line and the red line show pumping rate and wellhead pressure, respectively. The occurrences of AE events are indicated by vertical bars with different height, which correspond to relative magnitudes of the AE events. The wellhead pressure increases rapidly just after the pumping started. The first AE event was recorded during the 1st step rate injection at the pressure of 33MPa, which is close to the fracture pressure at the reservoir depth. The AE activity became active with increasing the injection rate. The activity hit a peak during the high-rate injection stage and the event rate reached 3 to 4 events per minute. The AE activity continued for approximately 2 hours after stop pumping. In the 2nd step-rate injection stage, the AE activity resumed when the injection rate increased to 2.0 BPM (5.3 l/s).

During the injection period, two notable pressure breakdowns were observed. The first is during the 1st step-rate injection stage and the 2nd is during the high-rate injection stage. The enhancement of the injectivity of the well is clear in the change of the pressure profiles between 1st step-rate injection and 2nd step-rate injection.

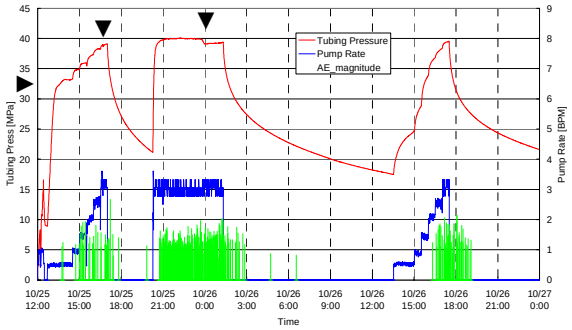

Figure 6: Pumping history and AE activity during the hydraulic injection experiment in the Yufutsu gas reservoir in 2003. ▼denotes the pressure breakdown. ►denotes the corresponding fracture pressure (≅σ3).

3.2 DFN Model

A DFN model is constructed by following the procedure proposed by Tamagawa et al., (2000) using the statistical properties of the fractures obtained from the micro-resisitivity images of the boreholes. A total of approximately 7,500 meter of micro-resistivity images from 12 wells in the Yufutsu field were investigated to derive the statistics, such as aperture, size, orientation and location distribution of fractures. The DFN model used for the study is a sector model extracted from the whole reservoir model. The sector model has a dimension of 1.5km by 1.5km by 1.5km and includes approximately 430,000 of fractures, whose radius ranges from 18m to 500m. Figure 7 shows the permeability distribution along the east-west cross section of the whole reservoir model with the close-up of the sector model used for the study.

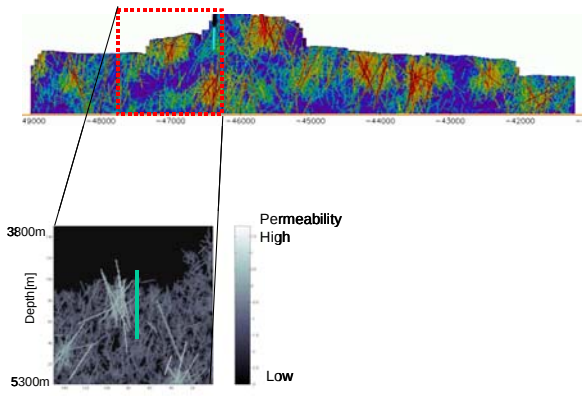

Figure 7: Permeability distribution along the east-west cross section of the whole reservoir model and the close-up of the sector model used for the study.

3.3 Pressure Matching Simulation

We tried to achieve a pressure matching using the SHIFT with inputs of the DFN model and the history of the injection rate. In the equivalent-continua model, the grid size is 4m × 4m × 50m around the injection well and is 50m × 50m × 50m near the outer boundary. The parameters for the rock and fluids properties are listed in Table 1.

The pressure at the 1st step-rate injection shows the curve with rapid increase at the initial period followed by the moderated increases according to the step-up injection. The significant change in the trend appears with the injection pressure reaching the corresponding fracture pressure (≅σ3), where the fractures around the borehole start to open. Through the simulation, it is found that the 10Mpa of *B* (90% closure stress) gives a good matching at this stage. Then, many times of try-and error processes are applied to get a good matching at the high rate injection stage and the 2nd step-rate injection stage by changing the other parameters such as fracture porosity, matrix porosity and the shear dilation angle. As the results of a number of iterations, it is found that the tuning of these parameter cannot reproduce the pressure response for the both stages simultaneously, while it reproduces only the pressure response during the high-rate injection stage. As shown in Figure 8, the simulated pressure responses at the 2nd step-rate injection stage show higher values than those at the 1st step-rate injection stage, in spite that the field data shows a significant decreases. This discrepancy may come from an underestimation of the effect of shearing to the permeability enhancement. The increase of simulated pressure is due to the increase of averaged pressure over the area where the injected water migrated and the replacement of the highly compressive gas with the low compressive water. The effect of shearing should be large enough to overcome these positive effects.

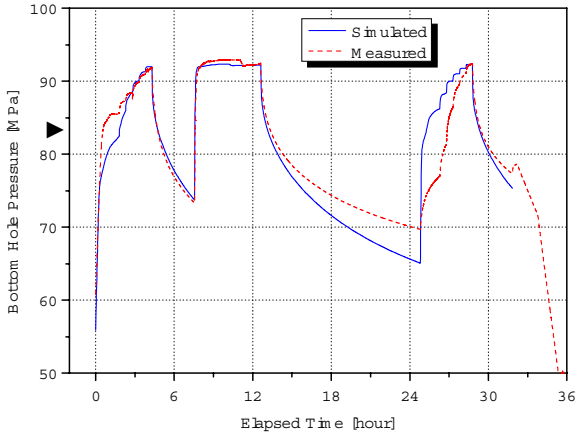

Figure 8: Intermediate results of the pressure matching with constant value of 90% closure stress. ▶denotes the estimated fracture pressure (≅σ3).

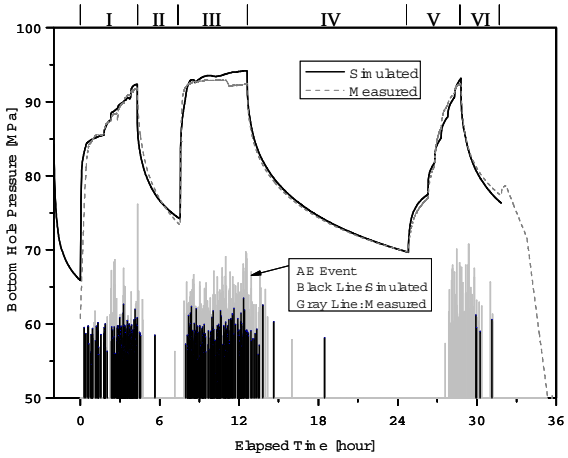

Figure 9: The best pressure matching with the parameters listed in Table2.

There are two options to enlarge the effect of shearing to permeability enhancement. The one is to take a larger value of the shear dilation angle and make the effect of shearing larger directly. The larger shear dilation angle, however, provides the effect uniformly to all the sheared fractures, regardless the pore pressure, which controls the effective normal stress facing to the fractures. Thus, the larger shear dilation angle suppresses the pressure during the high-rate injection stage as well. The other option is to make *B* (90% closure stress) higher. The higher *B* makes it difficult to close fractures with decreasing pore pressure. If we can take a higher *B* value only for the fractures that have arise shearing, it would be possible to lower the pressure at the 2nd step-rate injection stage with keeping the pressure at the high-rate injection stage high.

Figure 9 shows the best matching curve achieved after a number of try-and-error processes. The simulated curve shows good matching with the field data throughout the 1st step-rate injection, the high-rate injection and the 2nd step-rate injection. The pressure fall off after the high-ate injection also show good matching. The parameters that give the best matching are listed in Table 2. The *B* (90%

closure stress) value for the fracture after shearing is estimated ten times higher than that for the fractures before shearing.

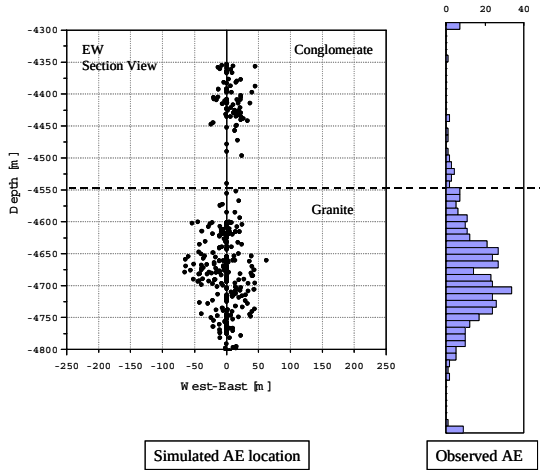

Figure 10: Comparison between the simulated AE event locations and the observed AE distribution.

3.4 AE Activity

Gray and black bars in Figure 9 indicate AE events observed in the field experiment and in the simulation, respectively. Height of the bar corresponds to a relative magnitude of an AE event and those for the simulated events are scaled smaller so as to make it easy to compare with the field data.

Significant mismatches are seen in the 2nd step-rate injection stage, while a reasonable matching can be seen in the 1st step-rate and the high-rate injection stages. This is because of the Kaiser effects put into the simulator. A fracture once has generated shearing never makes slip after that in the simulation. However, there may be repeated shearing in the actual reservoir, probably due to the stress reallocation and changes in friction coefficient during shearing.

Figure 10 shows a comparison between the simulated AE locations and the observed AE distribution. Because only one monitoring station was installed approximately 2km above the injection point, the uncertainty of the event location analysis is larger in horizontal direction than vertical direction. Thus, event histogram along the borehole, that includes only the vertical information, is used for the comparison. Most of events are concentrated in the granite section in the field observation. This tendency is consistent with the simulated event locations, which shows large AE cloud in the granite section.

3.4 Permeability Enhancement

Figure 11 shows permeability distribution around the well before and after injection. Following to the simulated results, the permeability around the injection well becomes ten to one hundred times larger than before injection.

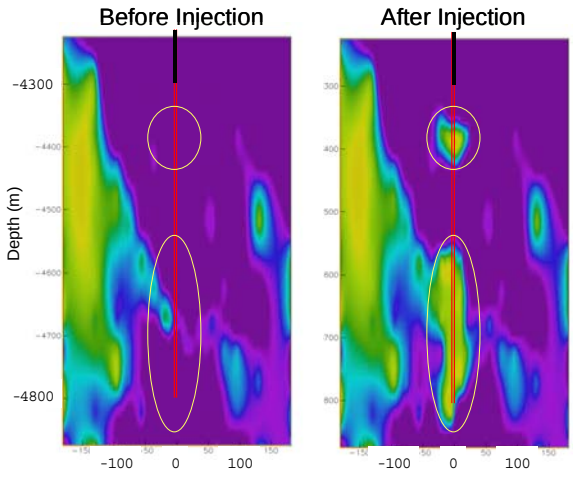

Figure 11: Permeability distribution around the well before and after injection.

4. DISCUSSION

The pressure matching shown in Figure 9 was obtained through a number of try-and-error processes by tuning the parameters. It is not easy task to get a good matching in the simulation, because many kinds of parameters have uncertainty and they affect the reservoir performances different ways. Followings are understandings about the sensitivity of each parameter obtained through the try and error processes, which may be helpful to get a better solution for further studies.

The injection period is divided into 6 stages as shown in Figure 9, so that the effect of each parameter, listed in Table 1 and 2, should be discussed clearly.

Stage I:

Pressure build up is sensitive to the grid configuration and the fracture distribution along the injection well. Pressure changes associated with the step up of the injection rate are controlled by shear dilation angle and 90% closure stress, especially in the range exceeding the fracture pressure.

Stage III:

Once a good matching has been obtained in stage I, the pressure during stage II shows a reasonable value. The degree of pressure breakdown is controlled by shear dilation angle and the size distribution of fracture.

Stage V:

The pressure profile in this stage tells us how the permeability has been increased by the past injection. The most sensitive parameter is the 90% closure stress for the sheared fracture. Fracture porosity is also sensitive because it governs the special extension of the sheared region.

Stage II, IV, VI:

Pressure fall off behaviors are strongly affected by parameters determining double-porosity model (ϕ_f and k_m). Larger the fracture fraction and smaller the matrix permeability, more gentle the pressure decline becomes.

5. CONCLUSION

The numerical simulator "SHIFT", which calculates performances of fractured basement reservoirs during hydraulic stimulations, has been developed. SHIFT simulates the shearing of fracture and relating AE activity and permeability enhancement in a dynamic process by coupling the fluid flow analysis and the shear dilation analysis. The performance of SHIFT was evaluated and verified through the case study using the field data from the hydraulic injection experiment in Yufutsu field. The simulated pressure curves shows a good matching to the field data with tuned-up parameters. The knowledge about the sensitivity of each parameter obtained through the matching processes is helpful to get a better solution for further studies.

SHIFT is useful to design an injection schedule for reservoir stimulation and to predict the effects of the stimulation, including a special extent of the stimulated area and a degree of permeability enhancement. SHIFT can be also used for evaluations of fracture network models and stress conditions; those are input parameters in the SHIFT, by comparing simulated results and field observations.

We will continue to verify and modify the functions of SHIFT by applying it to the past and the ongoing HDR projects.

ACKNOWLEDGMENTS

The authors would like to thank Japan Petroleum Exploration Co., Ltd. for permission to publish the data from the Yufutsu field, within this paper. The hydraulic injection experiment in Yufutsu field is supported by Japan Oil, Gas and Metals National Corporation (JOGMEC).

REFERENCES

Baria, R., and Green A. S. P.: Seismicity induced during a viscous stimulation at the Camborne School of Mines hot dry rock geothermal energy project in Cornwall, England, in Progress in acoustic emission, Yamaguchi, K., Aoki, K. and Kishi, T. Eds., *The Japanese Soc. for NDI*, (1986), 407-429.

Beauce, A., Jones, R., Fabriol, H., and Hulot, C.: Seismic studies on the Soultz HDR Project (France) during Phase IIa, *Geothermal Science and Technology*, **4**, (1995), 253-272.

Gerard, A., Baumgartner, J., Baria, R., and Jung, R.: An Attempt towards a Conceptual Model Derived from 1993-1996 Hydraulic Operations at Soultz. *Procedings*, of NEDO International Geothermal Symposium, Sendai, Japan, March 11-12, (1997), 329-341.

House, L.: Locating Microearthquakes Induced by Hydraulic Fracturing in Crystalline Rock, *Geophys. Res. Lett.*, **14 a**. (1987).

Ito, T. and Hayashi, K.: Role of Stress Controlled Flow Pathways in HDR Geothermal Reservoirs, *Pure and Applied Geophy*, **160**, (2003), 1103-1124.

Jing, Z., Willis-Richards, J., Watanabe, K. and Hashida, T.: A Three-dimensional Stochastic Rock Mechanics Model of Engineered Geothermal System in Fractured Crystalline Rock, *J. Geophys. Res.*, **105** (B10), (2000), 23, 663-23,679.

Jupe, A. J., Green, A. S. P., and Wallroth, T.: Induced microseismicity and reservoir growth at Fjallbacka hot dry rocks project, Sweden, *Int. J. Rock Mech. Min. Sci. & Geomech. Abst.*, **29**, (1992), 343-354.

Nagai, M. and Tenma, N.: Development of Hot Dry Rock Technology at Hijiori Test Site – Program for a Long Term Circulation Test, *Proceedings* of NEDO International Geothermal Symposium, Sendai, Japan, March 11-12, (1997), 351-356.

Narayan, S. P., Rahman, S. S., Jing, Z.: Proppant Free-Shear Dilation An Emerging Technology for Exploiting Tight to Ultra-Tight Gas Resources, SPE49251 presented at the 1998 SPE Annual Technical Conference and Exhibition, (1998).

Pearson, C.: The relationship between microseismicity and high pore pressure during stimulation experiments in low permeability granitic rocks, *J. Geophysical Res.*, 86, (1981), 7855-7864.

Pine, R. J. and Batchelor, A. S.: Downward migration of shearing in jointed rock during hydraulic injections. *Int. J. Rock Mech. Min. Sci. Geomech. Abstr*. **21**(5), (1984), 249-263.

Sasaki, S.: Characteristics of microseismic events induced during hydraulic fraturing experiments at Hijiori hot dry rock geothermal energy site, Yamagata, Japan, Tectonophysics, **289**, (1998), 171-188.

Talebi, S., and Cornet, F.H., Analysis of the microseismicity induced by a fluid injection in a granitic rock mass, Geophysical Research Letters, **14** (3), (1987), 227-230.

Tamagawa, T., Matsuura, T., Anraku, T., Tezuka, T. and Namikawa, T.: Construction of Fracture Network Model Using Static and Dynamic Data, SPE77741 presented at the 2002 SPE Annual Technical Conference and Exhibition, San Antonio, Txas, U.S.A., (2002).

Tester, J. W., Brown, D. W. and Potter, R. M.: Hot Dry Rock Geothermal Energy – A New Energy Agenda for the 21th Centry. Los Alamos Report LA-11515-MS. (1989).

Tezuka, K. and Niitsuma, H.: Stress estimated using microseismic clusters and its relationship to the fracture system of the Hijiori hot dry rock reservoir. *Engineering Geology*, **56**, (2000), 47-62.

Tezuka, K. and Watanabe, K.: Fracture Network Modeling of Hijiori hot dry rock reservoir by Deterministic and Stochastic Crack network simulator (D/SC), *Proceedings*, WGC 2000, (2000), 3933-3938.

Wallroth, T., Jupe, A. J., and Jones, R. H.: Characterisation of a fractured reservoir using microearthquakes induced by hydraulic injections, *Marine and Petroleum Geology*, **13** (4), (1996), 447-455.

Willis-Richards, J., Watanabe, K. and Takahashi, H.: Progress toward a Stochastic Rock Mechanics Model of Engineered Geothermal System, *J. Geophys. Res.*, **101**, (1996), 17,481-17,496.

Table 1: Input parameter used in simulation

Volume for simulation	
X Direction [m]:	-206 □ 206
Y Direction [m]:	-206 □ 206
Depth [m]:	-4200 □ -4900
Specification of injection well	
Location (X, Y):	(0,0)
Injection Zone [m]:	-4300 □ -4800
Rock properties	
Young's modulus [GPa]:	50
Poisson's ratio:	0.25
Total Porosity:	0.006
Rock fracture properties	
Static friction angle [deg.]:	38.66
Dynamic friction angle [deg.]:	11.31
Water properties	
Density [kg/m^3]:	$4.9075\times10^{-7}\times$Pressure [Pa] + 1180
Viscosity [Pa□s]:	2.5700×10^{-4}
Gas condensation properties	
Density [kg/m^3]:	$2.2694\times10^{-6}\times$Pressure [Pa] + 237
Viscosity [Pa□s]:	5.0829×10^{-4}

Table 2: Parameters estimated from pressure matching

In-situ stress state	
Vertical stress [MPa]:	0.0256×Depth [m]-11.8
Maximum horizontal stress [MPa]:	0.0314×Depth [m]+8.76
Minimum horizontal stress [MPa]:	0.0153×Depth [m]+8.76
Complex fracture opening properties	
Shear dilation angle [deg.]:	0.02
90% closure stress before shearing [MPa]:	10
90% closure stress after shearing [MPa]:	100
Properties of double porosity model for fluid flow analysis	
Fraction of fracture porosity to the total porosity:	0.25
Matrix Permeability [md]:	1×10^{-5}